



## Research paper

# Adaptive neuro-fuzzy inference system (ANFIS) approach for the irreversibility analysis of a domestic refrigerator system using LPG/TiO<sub>2</sub> nanolubricant



Jatinder Gill<sup>a,\*</sup>, Jagdev Singh<sup>b</sup>, Olayinka S. Ohunakin<sup>c,d</sup>, Damola S. Adelekan<sup>c</sup>, Opemipo E. Atiba<sup>c</sup>, Mojisola O. Nkiko<sup>e</sup>, Aderemi A. Atayero<sup>c,f</sup>

<sup>a</sup> Department of Mechanical Engineering, IKGPTU, Kapurthala, Punjab, India

<sup>b</sup> Faculty of Mechanical Engineering Department, BCET Gurdaspur, Punjab, India

<sup>c</sup> The Energy and Environment Research Group (TEERG), Mechanical Engineering Department, Covenant University, Ota, Nigeria

<sup>d</sup> Senior Research Associate, Faculty of Engineering and the Built Environment, University of Johannesburg, Johannesburg, South Africa

<sup>e</sup> Department of Physical and Chemical Sciences, Elizade University, Ilara Mokin, Nigeria

<sup>f</sup> IoT-Enabled Smart and Connected Communities (SmartCU) Research Cluster, Department of Electrical and Information Engineering, Covenant University, Ota, Nigeria

## ARTICLE INFO

## Article history:

Received 22 October 2019

Received in revised form 13 May 2020

Accepted 19 May 2020

Available online 28 May 2020

## Keywords:

LPG

ANN

TiO<sub>2</sub> nanoparticle

Total irreversibility

ANFIS

2nd law efficiency

## ABSTRACT

This work presents an adaptive neuro-fuzzy inference system (ANFIS) artificial intelligence methodology of predicting the 2nd law efficiency and total irreversibility of a refrigeration system running on LPG/TiO<sub>2</sub>-nano-refrigerants. For this purpose, subtractive clustering and grid partition approaches were utilized to train the ANFIS models required in estimating the 2nd law efficiency and total irreversibility using some experimental data. Furthermore, predictions of ANFIS models with subtractive clustering approach was found to be more accurate than ANFIS models predictions with grid partition approach. The predictions of ANFIS models with subtractive clustering approach were also compared with experimental results that were not included in the model training and predictions of already existing ANN models of authors previous publication. The comparison of variance, root mean square error (RMSE), mean absolute percentage error (MAPE) were 0.996–0.999, 0.0296–0.1726 W and 0.108–0.176 % marginal variability values. These results indicate that the ANFIS model with subtractive clustering approach having cluster radii 0.7 and 0.5 can predict the 2nd law efficiency and total irreversibility respectively, with higher accuracy than authors' previous publication ANN models.

© 2020 The Authors. Published by Elsevier Ltd. This is an open access article under the CC BY-NC-ND license (<http://creativecommons.org/licenses/by-nc-nd/4.0/>).

## 1. Introduction

Conventional approaches (i.e. analytical and experimental), have been used by various researchers to study energy and exergy features of conventional refrigerators (See [Ahamed et al., 2010](#); [Adelekan et al., 2017](#); [Gill and Singh, 2017a](#); [Saravanakumar and Selladurai, 2014](#); [Ahamed et al., 2011](#); [Raveendran and Sekhar, 2017](#); [Ohunakin et al., 2017, 2018](#); [Golzari et al., 2017](#); [Gill and Singh, 2017b](#); [Gill et al., 2018a,b,c, 2019](#); [Okotie et al., 2019](#); [Olatunji et al., 2019](#); [Onakade et al., 2019](#); [Akinlesi et al., 2019](#)). However, analytical approaches involve many theoretical assumptions and complex analytical estimations, while experimental studies are costly and time-consuming. Despite these challenges, artificial intelligence methods (especially artificial neural network (ANN) and adaptive neuro-fuzzy inference system

(ANFIS)) are extensively adopted in the field of refrigeration systems over the past few years ([Sowparnika et al., 2015](#); [Gill and Singh, 2017b](#); [Gill et al., 2018a](#)). Artificial intelligence approaches have shorter development, excellent approximation capabilities, and fast processing time. Numerous studies have adopted ANN numerical models in estimating refrigerator performances. [Esen et al. \(2008\)](#) used a minimum input data-based ANN model to forecast the operations of an experimental recoupled heat pump. It was concluded that the ANN model predicted the thermal system's coefficient of performance (COP) accurately. In another study, [Tong et al. \(2010\)](#) examined the behavior of a refrigerator by applying a three-input data-based ANN model. It was suggested that the model supports the creation of improved energy-efficient refrigeration systems operating under partial load conditions. According to the work of [Onder \(2011\)](#), an ANN model developed with a small set of data could determine the performance relative to some thermodynamic characteristics and energy consumption of a refrigeration system. The results of their

\* Corresponding author.

E-mail address: [gillzy1985@gmail.com](mailto:gillzy1985@gmail.com) (J. Gill).

### Nomenclature

I	Irreversibility, kW
ANFIS	Adaptive neuro fuzzy inference system
T	Temperature K
ANN	Artificial neural network
W	Compressor power kW
LPG	Liquefied petroleum gas
$M_r$	LPG refrigerant charge, g
$C_N$	Nanoparticle concentration, g/L
POE	Polyol ester oil
MO	Mineral oil

### Greek Letters

$\eta_{ex}$	2nd law efficiency (%)
-------------	------------------------

### Subscripts

total	Total
evap	Evaporator
cond	Condenser

predictions correlated perfectly with real values. Li et al. (2012) also employed an ANN simulation method to a direct expansion air-conditioner having about 169 experimental datasets. The developed ANN model accurately and simultaneously monitored temperature and humidity within the test room. Furthermore, Belman-Flores et al. (2013) designed a novel and advanced artificial intelligence model based on a near-exact quantification of neurons in the hidden layer for refrigeration systems. The model excellently estimated the energetic performances of the investigated refrigeration systems. Additionally, they recommended a fresh tool based on neural networks and capable of mapping the energy variability of a vapor compression refrigerator driven on R1234yf refrigerant. These maps could also determine the best performance zones (Ledesma and Belman-Flores, 2014). In a subsequent study by Belman-Flores and Ledesma (2015), a 3D graphic was built to visualize the stability of energy characteristics where input operating parameters were altered. An ANN model was developed for the high and low cycles of a cascade vapor compression refrigeration system (VCRS) using R134a refrigerant by Hosoz and Ertunc (2016). The model accurately predicted the energetic parameters of the entire cascade VCRS and the outcomes inferred it can alternatively and reliably model the system's performance. Furthermore, Rashidi et al. (2017) tried an artificial neural network-based methodology to predict unknown performance data of an ejector cooling cycle. Myriads of scholarly reports determined that the benefits of the ANN-based methodology amidst other methods, noting simplicity and faster operation. Gill and Singh (2018a) used ANN modeling techniques to predict the mass flow of R134a/LPG refrigerant in different adiabatic capillary tube geometries (i.e. straight and helical) of a VCRS. ANN model results adequately predicted the refrigerant mass flow rates with superior conventional dimensionless correlation and its results fitted closely to the experimental results. In addition, Gill et al. (2018c) proposed ANN models with four input parameters for evaluating some exergetic performance variables of a domestic refrigerator with LPG as a refrigerant and TiO<sub>2</sub>-Mineral oil. The experimental parameters predicted by the ANN models agreed well with experimental results especially for data that not configured by ANN models.

ANFIS approach combines the computational capabilities of ANN and fuzzy logic, which makes the ANFIS approach more accurate than ANN and Fuzzy logic techniques (See Hosoz et al.,

2011). Thus, many other researchers have adopted ANFIS approach to model various thermal systems parameters (See Hosoz et al., 2011; Yaici and Entchev, 2016; Gill and Singh, 2017c,d,e, 2018b). All researchers asserted that the ANFIS model predicted results of experiments with very high accuracy.

In a study carried out by Gill et al. (2018c), ANN models were used to predict the irreversibility and 2nd law efficiency of a domestic refrigerator working with LPG-TiO<sub>2</sub> mineral-oil blend of nanorefrigerant. Also, the authors claimed that the numerical ANN approach predicted the performances accurately. Besides, the predictions correspond to experimental findings not previously utilized in preparing the ANN models. Given the conclusion by Hosoz et al. (2011), that ANFIS based approaches are more accurate than ANN approaches, together with sparse information available in the literature on the use of ANFIS approach to predict the total irreversibility and 2nd law efficiency of domestic refrigerators charged with LPG refrigerant and TiO<sub>2</sub> based nanolubricating oil. Because of the high accuracy of ANFIS models when compared to other numerical models, this research work thus presents an ANFIS based irreversibility analysis of a domestic refrigeration system infused with LPG-TiO<sub>2</sub> nano-refrigerant. The irreversibility performance parameters chosen within this study were limited to 2nd law efficiency and total irreversibility of the refrigeration system. The recommended ANFIS models were trained, and the predictions were compared with the experimental values not included in model training and results of the ANN models developed by Gill et al. (2018c). The comparisons were based-on statistical parameters including R<sup>2</sup>, MAPE, and. RSME

## 2. Experimental procedure and setup

A complete depiction of the experimental setup (Fig. 1) and the procedure for assessing the total irreversibility and 2nd law efficiency within the test rig have been discussed in the earlier work of authors (see Gill et al., 2018c). Furthermore, this test rig was modified by placing the evaporator and condenser in insulated cabins as shown in Fig. 1. Table 1 shows the sub-component specification of the test rig. Variac controlled electrical resistances were installed within the cabins to adjust the internal temperature as required. The temperatures of the condenser and evaporator were maintained at the desired value by modifying the electrical resistance with the variac. Experimental data were captured for selected condenser temperatures, evaporator temperatures, and nanoparticle concentrations to estimate the total irreversibility and 2nd law efficiency. Experimental trials were conducted through separate fixing the condenser temperatures, evaporator temperatures, and nanoparticle concentrations while also monitoring their influences within the rig. For example, at a given value of evaporator and condenser temperatures (that is -16 °C and 34 °C respectively), and a change in the concentration of TiO<sub>2</sub> particles from 0 to 0.6 g/L, the total irreversibility and 2nd law efficiency were separately evaluated in line with the procedure described in Gill et al. (2018c). Similarly for another trial, the evaporator and the condenser temperatures were set separately, and the remaining parameters were changed, before evaluating the total irreversibility and second law efficiency again. Furthermore, all experimental trials were conducted using the optimal amount of LPG charge (40 g) already established in Gill et al. (2018d). Each experimental trial was repeated three times and mean values adopted. The uncertainty of measured parameters are as shown in Table 2.

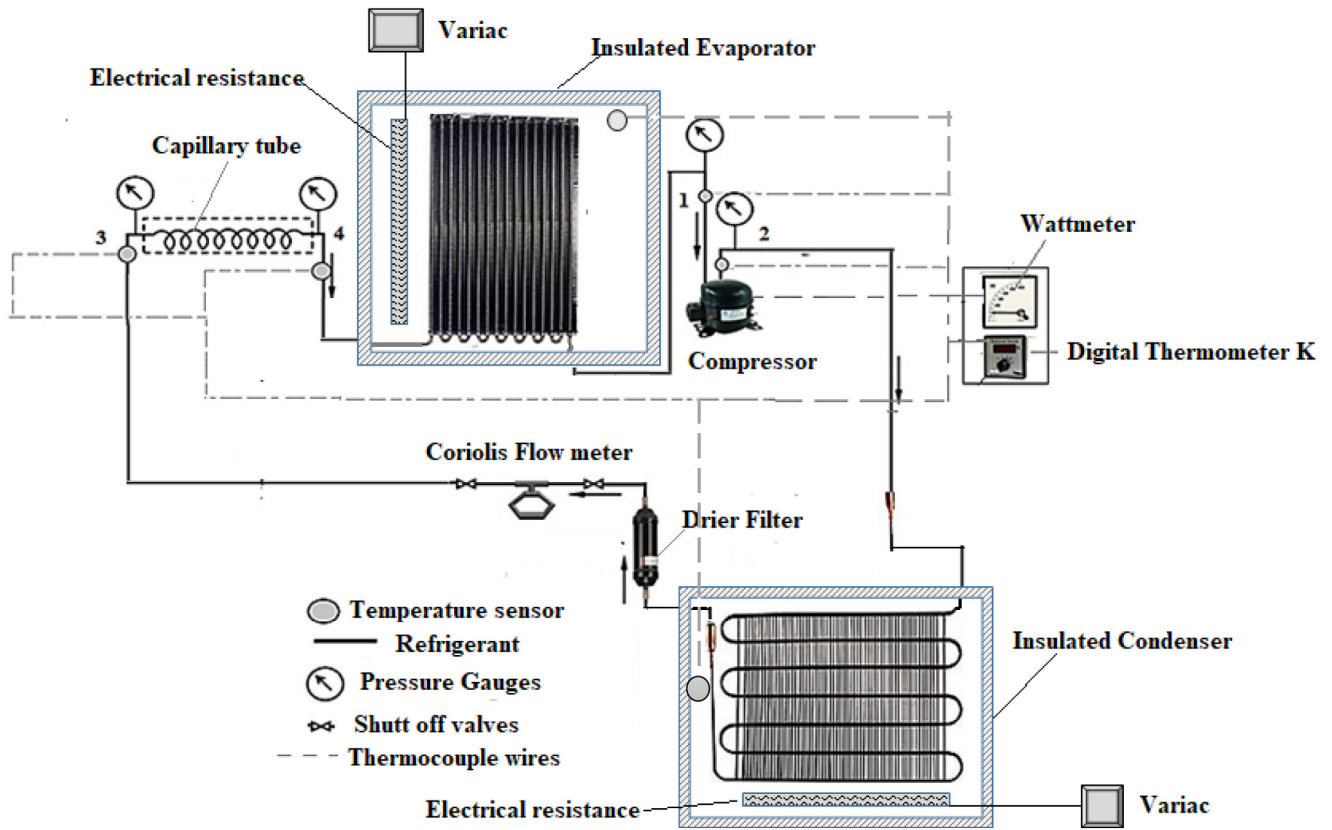


Fig. 1. Schematic diagram of experimental setup.

**Table 1**  
Test rig subcomponent specification.

S/N	Description	Unit
1	Capillary tube length	2 m
2	Condenser type	Air cooled (Condenser tube diameter 6.35 mm)
3	Evaporator size	62 L (Evaporator tube diameter 6.4 mm; length 7.62 m)
4	Compressor type	HFC
5	Refrigerant mass charge	100 g
6	Type of refrigerant	R134a (HFC class)
7	Power rating	110 W
8	Number of doors	Single
9	Voltage rating	220–240 V

**Table 2**  
Uncertainty of measured parameters.

S/N	Parameter	Absolute uncertainty ( $\pm$ )
1	$\eta$	1.93%
2	$P_1, P_4$	2 kPa
3	$P_2, P_3$	2 kPa
4	$T_1$	0.2 °C
5	$T_2$	0.2 °C
6	$T_3$	0.2 °C
7	$T_4$	0.2 °C
8	$I_{total}$	2.79 W

### 3. ANN and ANFIS modeling

#### 3.1. ANN modeling

Artificial neural network (ANN) exploits biological process based computational method to solve complex problems too

tedious for humans or computers. ANNs are assumed to be black-box, due to its sets of outputs and inputs. Also, ANNs can be adapted to a wide range of situations with no previously existing mathematical equation or model. According to [Ledesma and Belman-Flores \(2014\)](#), ANNs can be easily executable on both hard and soft wares. Software programs similar to MATLAB can be used to develop ANN models. The required number of neurons in each layer can be set accordingly. Neurons are essential component of an ANN used to process received-signals from other neurons to produce an output-signal. Individual neuron is a summation and activation functions. The activation functions is usually a continuous, real, positive derivative, limited and mostly sigmoid in shape. Typically, ANNs consists of input, output and hidden layers. The number of hidden layer with an ANN model is subject to its application. In a recent study by [Gill et al. \(2018c\)](#), The ANN model used for predicting the irreversibility performance of a domestic refrigeration systems utilized only one hidden layer; the configuration provided the best results. The architecture of one hidden layer based artificial neural network used in [Gill et al. \(2018c\)](#), can be found in [Fig. 2](#). In the same work of [Gill et al. \(2018c\)](#), two ANN networks were prepared, and each network had four inputs namely: condenser temperature ( $T_{cond}$ ), evaporator temperature ( $T_{evap}$ ), nanoparticle concentration ( $C_n$ ), LPG charge ( $M_R$ ), and one output parameter (i.e. total irreversibility and the 2nd law efficiency of domestic refrigerator) for each scenario. [Gill et al. \(2018c\)](#) proposed Eqs. (1)–(2), to assess the total irreversibility and 2nd law efficiency of the domestic refrigeration system charged with LPG refrigerant and TiO<sub>2</sub> based lubricant.

$$I_{total} = \left[ \frac{2}{(1 + e^{-2*(E_{11})_{total}})} - 1 \right] \quad (1)$$

$$\eta_{ex} = \left[ \frac{2}{(1 + e^{-2*(E_{11})_{ex}})} - 1 \right] \quad (2)$$

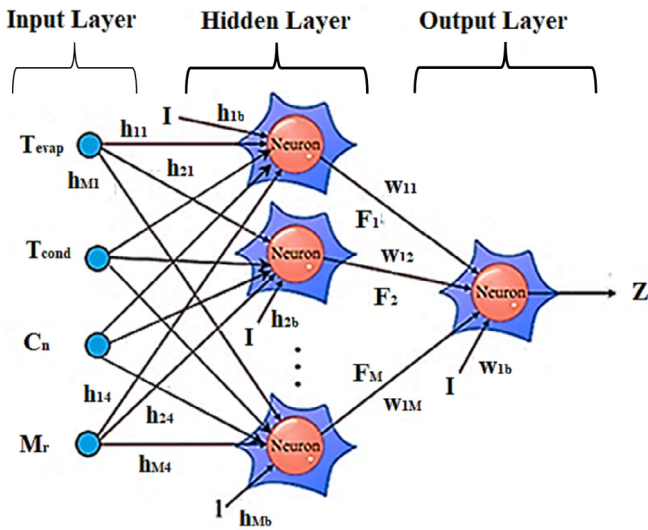


Fig. 2. Artificial neural network (Gill et al., 2018c).

If ( $A_1$  is  $x$ ) & ( $B_1$  is  $y$ ); then ( $z_1 = r_1 + q_1 y + p_1 x$ ) Rule 1  
 If ( $A_2$  is  $x$ ) & ( $B_2$  is  $y$ ); then ( $z_2 = r_2 + q_2 y + p_2 x$ ) Rule 2

In Rule 1 and Rule 2 above,  $A_i$  and  $B_i$  represents fuzzy sets,  $Z_i$  is the output around the fuzzy area stated by fuzzy rules while  $p_i$ ,  $r_i$ , and  $q_i$  are the obtained design parameters of the training process. ANFIS architecture implements these rules as represented in Fig. 3; the circle indicates a fixed node, while adaptive nodes were represented with the square symbols. Detailed information regarding ANFIS can be found in Gill and Singh (2017c,d,e).

A MATLAB R2017b software was used to run the ANFIS models of this study. In addition, the ANFIS models in this study had four and two input and output variables respectively. The four input variables were evaporator temperature ( $T_{Evap}$ , °C), refrigerant charge ( $M_R$ , g), nanoparticle concentration ( $C_N$ , g L<sup>-1</sup>) and condenser temperature ( $T_{cond}$ , °C). The output variables (that is Total irreversibility, and 2nd law efficiency) of the developed models were independently determined. The experimental data available in Gill et al. (2018c) served as the training database for the ANFIS models. However, in this study, instead of using conventional validation technique, leave-one-out cross-validation (typically abbreviated as LOOCV) was adopted to validate the configured ANFIS models. More information on LOOCV can be found in Gill et al. (2018c). Additionally, the versatility of the developed ANFIS models were valued by studying the influences of the input parameters ( $T_{evap}$ ,  $T_{cond}$ ,  $C_N$ ,  $M_R$ ) on the output parameters (total irreversibility and 2nd law efficiency).

As shown in the block diagram of Fig. 4, the ANFIS model were configured or trained in manner that predefined input lead to a specified output. The ANFIS model was trained by comparing the target and output in line with the expected goal.

To obtain optimized ANFIS model parameters, two approaches (that is, Grid partition with different number of Gaussian membership functions, and subtractive clustering with different cluster radius) were utilized for training the ANFIS models. In the subtractive clustering method, the data groups were represented in clusters to generate the fuzzy inference system. Different values of cluster radius (0.5 to 0.8) were utilized in the MATLAB program to identify the optimum number, and form the fuzzy rules. In the grid partition approach, various number of Gaussian membership functions (i.e. 3 to 5) were used to train the ANFIS models. The Gaussian membership function was selected for grid partition approach because of its higher prediction accuracy as described by Gill and Singh (2018b). Hybrid learning algorithm was adopted for the ANFIS model training on the basis of its high efficiency as asserted by Guler and Ubeyli (2005). Statistical variability characteristics such as mean absolute percentage error (MAPE),

where

$$(E_{11})_{total} = F_1 * (0.7193) + F_2 * (0.0012) + F_3 * (0.3928) + F_4 * (0.0445) + F_5 * (0.2438) + F_6 * (0.1773) + F_7 * (0.0072) + F_8 * (-0.0391) + F_9 * (-0.5103) + F_{10} * (-0.5867) + 0.4038 \quad (3)$$

$$(E_{11})_{ex} = F_1 * (-0.4642) + F_2 * (0.0463) + F_3 * (-0.6668) + F_4 * (-0.3193) + F_5 * (-0.2244) + F_6 * (-0.1981) + F_7 * (-0.1659) + F_8 * (0.0806) + F_9 * (-0.2036) + F_{10} * (0.3036) - 0.2563 \quad (4)$$

3.2. Adaptive neuro fuzzy inference system modeling

Jang (1993) developed the Adaptive Neuro Fuzzy Inference system. ANFIS is a multilayer feed-forward network comprising of nodes and directed links. ANFIS model operations depends on the fuzzy Sugeno model within the adaptive system framework to assist its learning and adaptation. The adaptive neuro-fuzzy inference framework allows the model to be less dependent on proficient knowledge and more systematic in its approach. For simplicity, we assumed that the fuzzy-logic inference system of interest had two inputs ‘x and y’ and one output ‘z’. Let the rule base contains two fuzzy “if-then” rules of Takagi and Sugeno’s type:

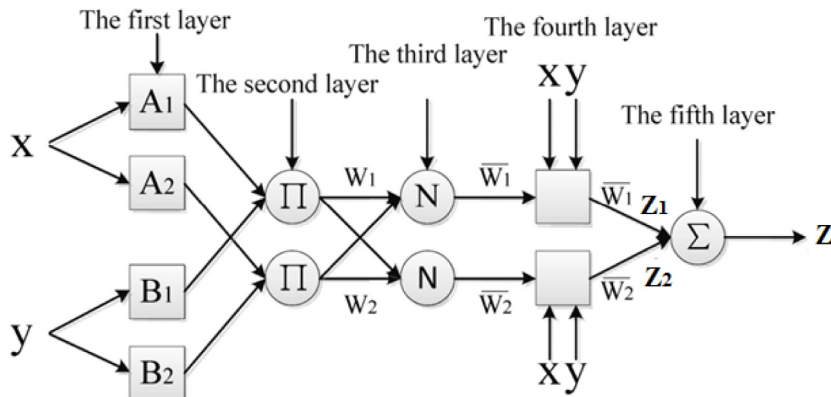
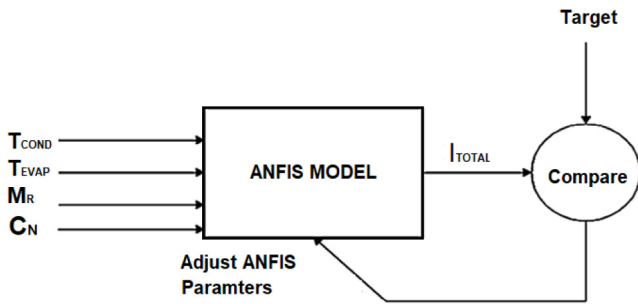


Fig. 3. ANFIS architecture with a two-input first-order Sugeno fuzzy model with two rules (Gill and Singh, 2017e).



**Table 3**  
Training error associated with each output parameter for ANFIS-SC and ANFIS-GP methodologies.

Methodology	Total irreversibility		Second law efficiency	
		Training error		Training error
ANFIS with Grid partition (ANFIS-GP) Gaussian Membership function	Number of Gaussian MF = 3 (rules = 81)	0.000121128	Number of Gaussian MF = 3 (rules = 81)	6.74192e−05
	Number of Gaussian MF = 4 (rules = 256)	4.57512e−05	Number of Gaussian MF = 4 (rules = 256)	3.95639e−05
	Number of Gaussian MF = 5 (rules = 625)	4.58512e−05	Number of Gaussian MF = 5 (rules = 625)	3.96504e−05
ANFIS with subtractive clustering (ANFIS-SC)	Cluster radius R = 0.5 (rules = 16)	2.68796e−05	<b>Cluster radius R = 0.5 (rules = 16)</b>	<b>1.6717e−05</b>
	Cluster radius R = 0.6 (rules = 11)	7.88477e−06	Cluster radius R = 0.6 (rules = 11)	7.153e−06
	<b>Cluster radius R = 0.7 (rules = 8)</b>	<b>1.60708e−06</b>	Cluster radius R = 0.7 (rules = 8)	2.8392e−06
	Cluster radius R = 0.8 (rules = 6)	0.000294439	Cluster radius R = 0.8 (rules = 6)	2.417e−06



**Fig. 4.** Block diagram of proposed ANFIS model for total irreversibility.

root mean square error (RMSE), and absolute fraction of variance ( $R^2$ ) were used to correlate the actual and predicted values not included in the training process. The least MAPE and RSME values, and maximum  $R^2$  value were the criteria selected to identify the optimum number and form of fuzzy rules in both approaches (See Gill and Singh (2017d), for the definitions of these statistical parameter).

**4. Results and discussions**

In this study, the experimental data used in Gill et al. (2018c) served as the database (144 dataset for training; 16 dataset for testing) for this ANFIS modeling. After the ANFIS models were trained, their performances were evaluated in terms of LOOCV technique. The total irreversibility and second law efficiency were the two parameters that were selected for validation using their relative error estimations. Furthermore, the performance results obtained from ANFIS models for the total irreversibility and second law efficiency were also compared with measured data and results of ANN models developed by Gill et al. (2018c), in terms of their statistical indices namely  $R^2$ , RMSE, and MAPE.

In order to obtain optimal model parameters, the ANFIS models were trained using Grid partition methodology with diverse number of Gaussian membership functions (3–5) and subtractive clustering methodology with different cluster radius (0.5–0.8); training error for each output parameter was evaluated. Table 3 shows the training error associated with each output parameter for both methodologies namely: Subtractive Clustering with

different cluster radius, and Grid Partition with different number of Gaussian membership functions. Table 3 shows that for the total irreversibility, the methodology with subtractive clustering of 0.7 cluster radius had the smallest training error, while for the second law efficiency the smallest training error was observed with 0.5 cluster radius using Subtractive Clustering methodology. Hence, ANFIS with Subtractive Clustering approach (ANFIS-SC) seems more accurate than ANFIS with Grid partition (ANFIS-GP), concerning modeling the total irreversibility and 2nd law efficiency. The membership plots for the selected input variables of the ANFIS-SC methodology are shown in Figs. 5(a)–5(d). It can be observed that the ANFIS-SC approach with a cluster radius of 0.7 and 8 rules predicted the total irreversibility of the domestic refrigeration system with high accuracy (see Table 3); we identified eight clusters having the Gaussian variation were identified (no rules = no clusters) for the selected input parameters. These eight clusters for the selected input parameters are as shown in Figs. 5a–d, where the abscissa and ordinate represent the selected range of input variables and the degree of membership associated with the cluster, respectively. In addition, the optimal number of rules required to model the total irreversibility and second law efficiency using ANFIS-SC methodology, were eight (8) and sixteen (16) respectively. ANFIS-SC rule viewers for predicting the total irreversibility and 2nd law efficiency are presented in Figs. 6(a)–6(b), while ANFIS-SC architecture for one of the output parameter ( $I_{total}$ ) is as shown in Fig. 7. In Figs. 6(a)–6(b), first four columns (starting from left to right) represent the cluster variation corresponding to the selected input variable, however the last column represent the predicted output of ANFIS-SC model. Since, ANFIS-SC approach with eight and sixteen clusters predicted the total irreversibility and second law efficiency with high accuracy respectively, then eight and sixteen rules were required as shown in Figs. 6(a)–6(b). It can thus be observed from these figures that if  $T_{Evap} = -16.38^\circ\text{C}$ ,  $T_{Cond} = 35.10^\circ\text{C}$ ,  $C_N = 0$  and  $M_R = 40\text{g}$  then  $I_{Total} = 45.4\text{W}$  and  $\eta_{ex} = 37.6\%$  respectively were predicted by the ANFIS-SC approach. After training the ANFIS models, the effectiveness of the trained models were evaluated by calculating the relative errors for the total irreversibility and 2nd law efficiency of a domestic refrigerator using the LOOCV technique.

Comparison of ANN and ANFIS-SC model predictions along with experimental results that were not used in developing the model for the operational variables ( $T_{evap}$ ,  $T_{cond}$ ,  $C_N$ ,  $M_R$ ) are as

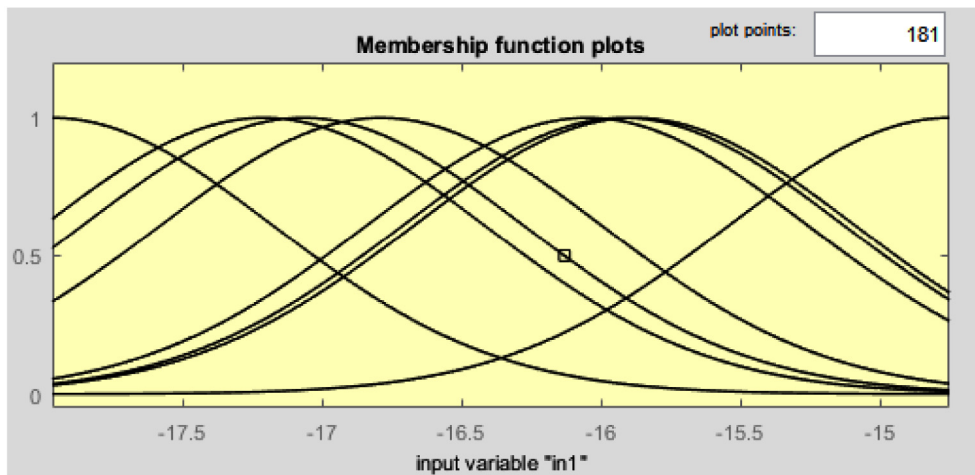


Fig. 5(a). Membership plot for the evaporator temperature as input variable.

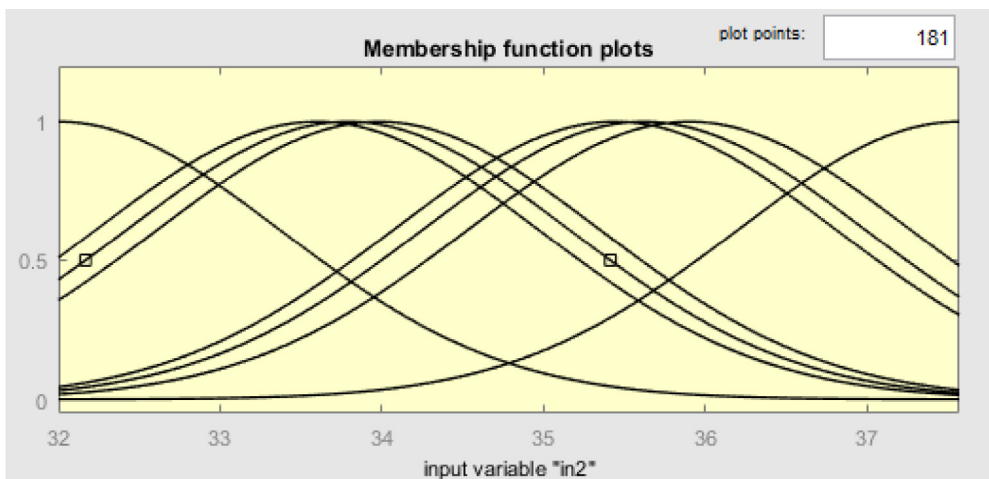


Fig. 5(b). Membership plot for the refrigerant charge as input variable.

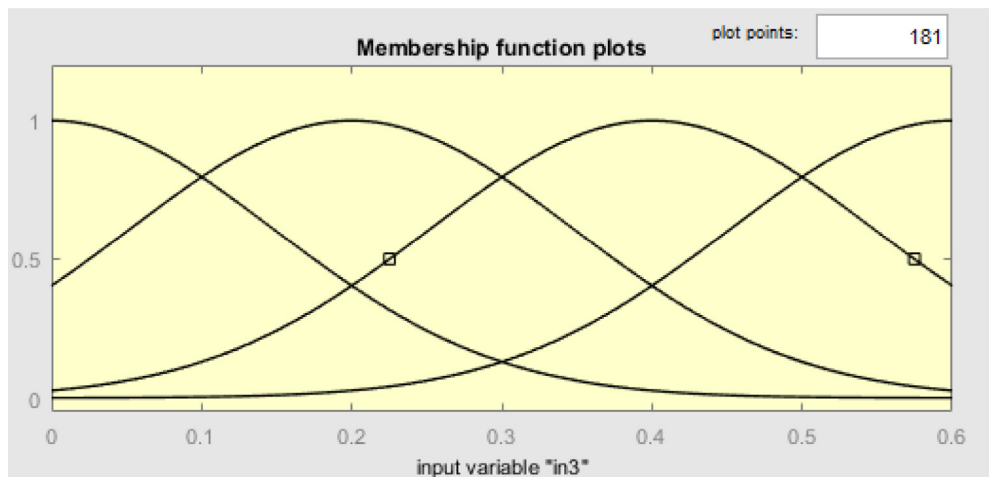


Fig. 5(c). Membership plot for the nanoparticle concentration as input variable.

indicated in Tables 4 and 5. Statistical indices ( $R^2$ , RMSE and MAPE) of the ANFIS-SC with different cluster radii and ANN models, based on experimental results were also evaluated in Tables 4 and 5. The ANFIS-SC ( $R = 0.7$ ) model predictions of total irreversibility and ANFIS-SC ( $R = 0.5$ ) model predictions of

second law efficiency, had the highest value of  $R^2$  and the smallest values of RMSE and MAPE, when compared with the ANFIS-SC models and the ANN model developed in Gill et al. (2018c). Hence, the total irreversibility of ANFIS-SC ( $R = 0.7$ ) model and the second law efficiency of ANFIS-SC ( $R = 0.5$ ) model, proved

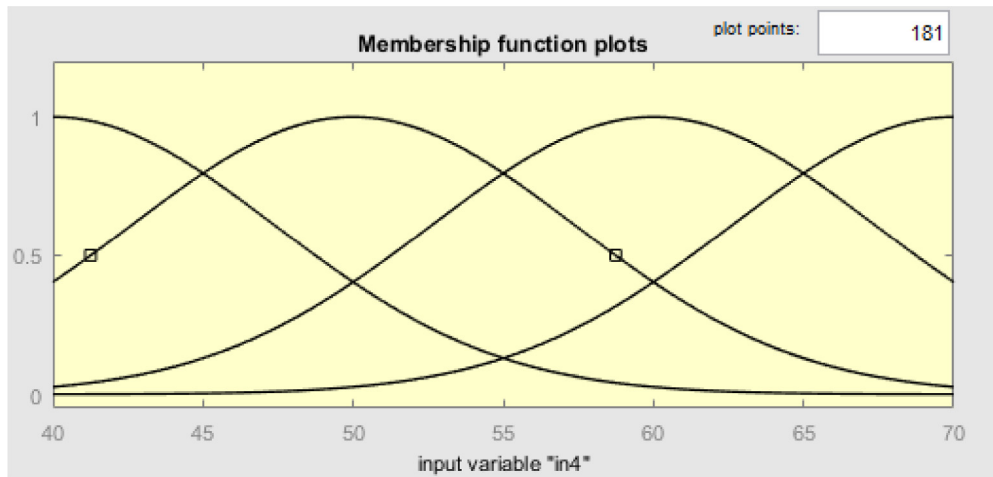


Fig. 5(d). Membership plot for the refrigerant charge as input variable.

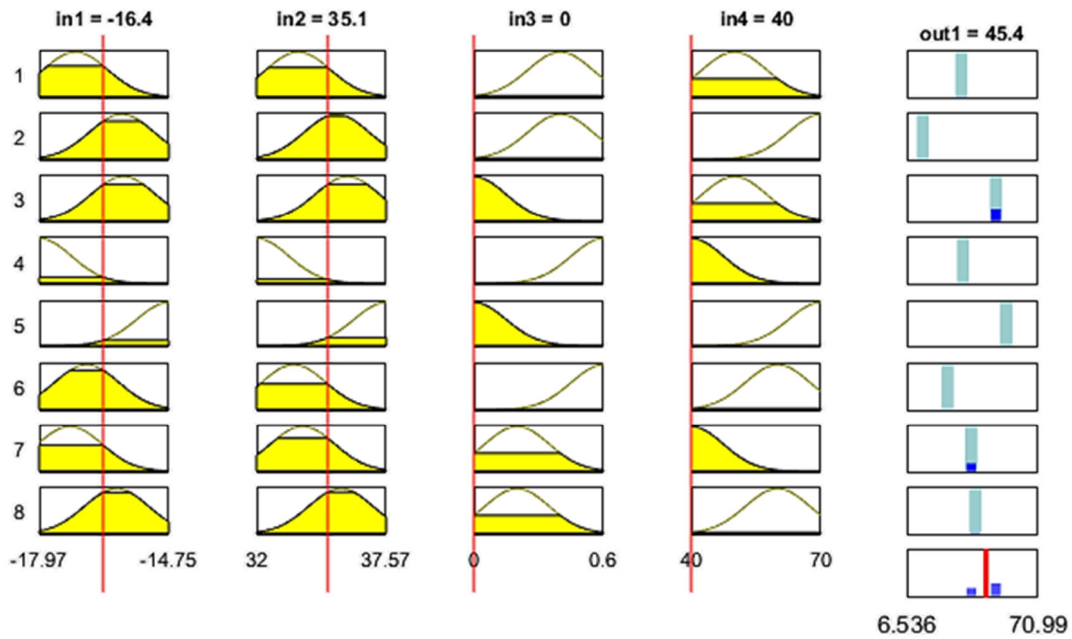


Fig. 6(a). ANFIS-SC rule viewers for predicting the total irreversibility.

to be most accurate in comparison to other ANFIS-SC models and ANN models earlier developed in the work of Gill et al. (2018c).

Based on the statistical performance results mentioned in Tables 4 and 5, the ANFIS-SC ( $R = 0.7$ ) model predictions of the total irreversibility and ANFIS-SC ( $R = 0.5$ ) model predictions of second law efficiency, compared to the experimental outcomes and the estimates of the ANN model as developed in the work of Gill et al. (2018c), are described in Figs. 8–9. The symmetrical straight line in Figs. 8 and 9 represent the experimental results. Figs. 8 and 9 show that the ANFIS-SC model predictions are closer to the experimental results, than the calculations of the ANN model, since the predictions of the ANFIS-SC models ( $R = 0.5$ ,  $R = 0.7$ ) gave higher  $R^2$  values and lesser RSME and MAPE values than the ANN models predictions of total irreversibility and 2nd law efficiency. Results of statistical analysis showed that the predictions of the ANFIS-SC models ( $R = 0.5$ ,  $R = 0.7$ ), for the 2nd law efficiency and total irreversibility yields  $R^2$ , RMSE and MAPE in the range of 0.998–0.999, 0.031–0.034 and 0.061–0.078% accordingly with respect to actual experimental data.

After the ANFIS-SC models were trained, their performances were evaluated in terms of their relative errors using LOOCV

technique as per Eq. (5). The total irreversibility and 2nd law efficiency were two key parameters selected for validation using the relative error of their estimations. Fig. 10 compared the relative errors of the total irreversibility and second law efficiency in accordance with the LOOCV method, for the proposed ANFIS-SC models and the ANN models developed by Gill et al. (2018c). The abscissa represents the validation sample (80 datasets), whereas ordinate represents relative error; both measurements had no units. The total irreversibility and second law efficiency parameters are displayed with red and blue colors respectively. The solid line represents a relative error variation using the ANFIS-SC models, while the dashed lines represents the relative error variation using the ANN models. Fig. 10 show that the relative errors of the total irreversibility and second law efficiency estimated from the ANFIS-SC models are lower than the ANN models. In addition, a maximum relative error of 0.019 was observed for the second law efficiency using the ANFIS-SC model; this is lesser than the maximum relative error for the ANN model. Furthermore, the ANFIS-SC models had more null relative errors as compared to ANN models (See Fig. 10). Hence, the proposed ANFIS-SC model

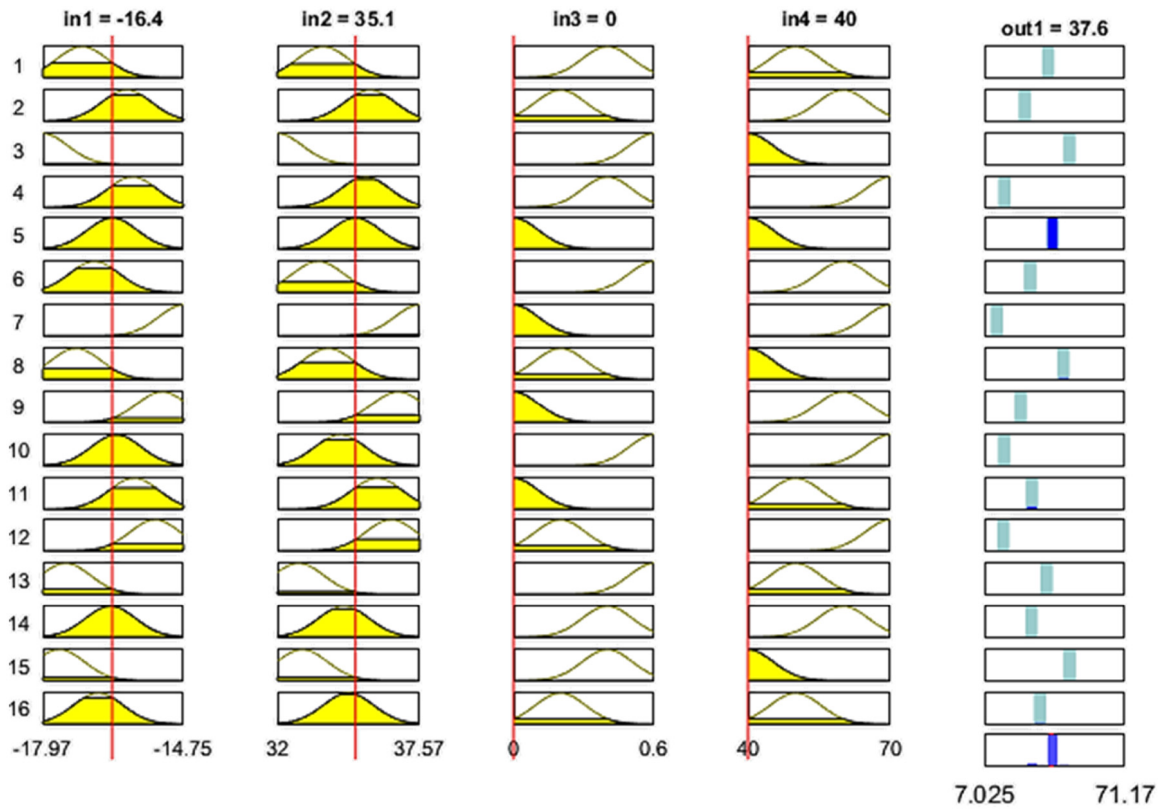


Fig. 6(b). ANFIS-SC rule viewers for predicting the second law efficiency.

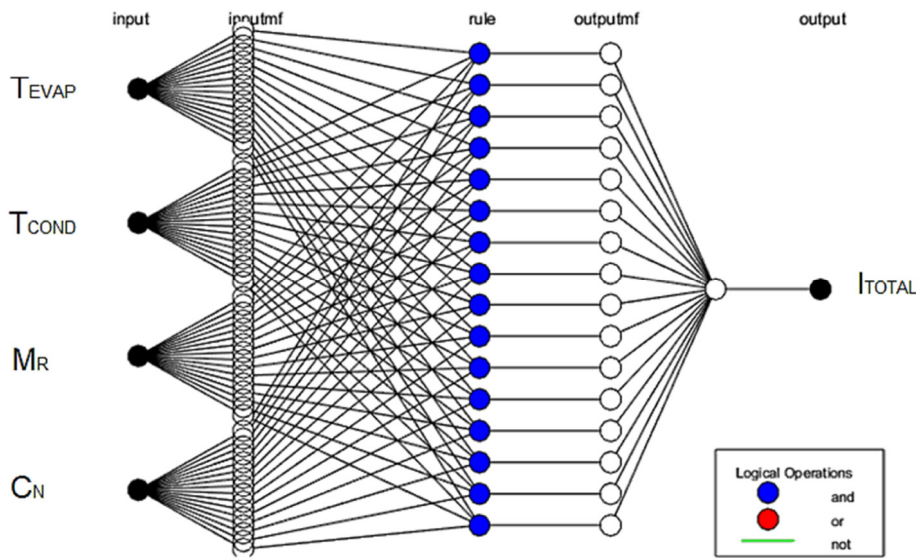


Fig. 7. ANFIS-SC architecture for total irreversibility as output parameter ( $I_{total}$ ).

is more accurate than the recently developed ANN models of the work of Gill et al. (2018c).

$$LOOCV \text{ error} = \frac{1}{N} \sum_{i=1}^N MSE_i \quad (5)$$

where MSE is known as Means square error

Furthermore, the versatility of the developed ANFIS SC models can be assessed by studying the influences of the input parameters ( $T_{evap}$ ,  $T_{cond}$ ,  $C_N$ ,  $M_R$ ) on the output parameters (total irreversibility and 2nd law efficiency). For this purpose, predictions

of the developed ANFIS-SC models for the total irreversibility and second law efficiency as a function of input parameters are presented in Figs. 11–17, as sample results. Figs. 11–14 indicate the predicted surface of ANFIS-SC for total irreversibility and 2nd law efficiency with respect to the two selected input parameters, while other input parameters were kept constant. In the figures (Figs. 11–14), the highest second law efficiency and smallest total irreversibility regions or vice versa can be easily identified, from the surface variation. However, Figs. 15–17 illustrate the ANFIS-SC predictions of total irreversibility and 2nd law efficiency with respect to one input parameter, while other input parameters



**Table 4**  
Comparison of ANN and ANFIS-SC models predictions of total irreversibility along with experimental results.

Sr No	Operating variables				Exp. (Gill et al., 2018c)	ANN (Gill et al., 2018c)	ANFIS with subtractive clustering (ANFIS-SC)			
	T <sub>evap</sub>	T <sub>cond</sub>	C <sub>N</sub>	M <sub>R</sub>			Cluster radius R = 0.5 (rules = 16)	Cluster radius R = 0.6 (rules = 10)	<b>Cluster radius R = 0.7 (rules = 8)</b>	Cluster radius R = 0.8 (rules = 6)
Total irreversibility (W)										
1	-16.38	35.06	0.00	40.00	45.40	44.33	45.10	45.30	<b>45.40</b>	45.50
2	-17.21	33.98	0.20	40.00	36.66	37.09	36.20	36.60	<b>36.70</b>	36.50
3	-17.59	32.97	0.40	40.00	34.46	34.71	34.40-	34.60	<b>34.50</b>	34.90
4	-17.97	32.00	0.60	40.00	34.36	34.46	34.30	34.50	<b>34.40</b>	34.60
5	-15.88	35.90	0.00	50.00	49.98	48.16	49.70	48.40	<b>50.00</b>	49.30
6	-16.70	34.78	0.20	50.00	40.80	41.31	41.70	40.80	<b>40.80</b>	40.90
7	-17.07	33.79	0.40	50.00	38.35	39.45	38.20	38.30	<b>38.40</b>	38.50
8	-17.45	32.83	0.60	50.00	38.10	38.90	38.00	38.20	<b>38.10</b>	38.20
9	-15.24	36.72	0.00	60.00	54.23	52.74	54.10	54.30	<b>54.20</b>	54.40
10	-16.05	35.62	0.20	60.00	45.22	44.56	45.20	45.30	<b>45.20</b>	45.20
11	-16.42	34.60	0.40	60.00	42.51	43.01	42.40	42.30	<b>42.50</b>	42.60
12	-16.79	33.60	0.60	60.00	42.02	42.47	42.00	42.10	<b>42.00</b>	42.20
13	-14.75	37.57	0.00	70.00	64.47	63.94	64.40	65.50	<b>64.50</b>	65.60
14	-15.40	36.45	0.20	70.00	53.31	53.15	53.20	53.50	<b>53.40</b>	53.40
15	-15.92	35.44	0.40	70.00	50.12	51.41	50.10	50.20	<b>50.10</b>	50.30
16	-16.29	34.46	0.60	70.00	50.02	50.04	50.00	50.10	<b>50.00</b>	50.20
<b>Statistical analysis</b>						R <sup>2</sup> = 0.990 RSME = 1.06 W MAPE = 1.734%	R <sup>2</sup> = 0.998 RSME = 0.28 W MAPE = 0.412%	R <sup>2</sup> = 0.996 RSME = 0.48 W MAPE = 0.501%	<b>R<sup>2</sup> = 0.999</b> <b>RSME = 0.034</b> <b>W</b> <b>MAPE = 0.061%</b>	R <sup>2</sup> = 0.998 RSME = 0.37 W MAPE = 0.533%

**Table 5**  
Comparison of ANN and ANFIS-SC models predictions of second law efficiency along with experimental results.

Sr No	Operating variables				Exp. (Gill et al., 2018c)	ANN (Gill et al., 2018c)	ANFIS with subtractive clustering (ANFIS-SC)			
	T <sub>evap</sub>	T <sub>cond</sub>	C <sub>N</sub>	M <sub>R</sub>			<b>Cluster radius R = 0.5 (rules = 16)</b>	Cluster radius R = 0.6 (rules = 11)	Cluster radius R = 0.7 (rules = 8)	Cluster radius R = 0.8 (rules = 6)
Second law efficiency (W)										
1	-16.38	35.06	0.00	40.00	37.57	37.72	<b>37.60</b>	37.20	37.40	37.30
2	-17.21	33.98	0.20	40.00	42.00	41.20	<b>42.00</b>	41.00	41.40	41.30
3	-17.59	32.97	0.40	40.00	44.21	43.75	<b>44.20</b>	43.60	44.30	44.40
4	-17.97	32.00	0.60	40.00	44.12	43.49	<b>44.10</b>	44.20	44.10	44.30
5	-15.88	35.90	0.00	50.00	33.50	35.71	<b>33.50</b>	33.60	33.40	33.60
6	-16.70	34.78	0.20	50.00	37.58	37.03	<b>37.60</b>	37.50	36.05	37.40
7	-17.07	33.79	0.40	50.00	40.95	39.77	<b>40.90</b>	41.10	41.10	40.80
8	-17.45	32.83	0.60	50.00	40.58	40.03	<b>40.60</b>	40.70	40.50	40.60
9	-15.24	36.72	0.00	60.00	30.35	32.45	<b>30.40</b>	30.20	30.50	30.30
10	-16.05	35.62	0.20	60.00	33.21	32.91	<b>33.20</b>	33.10	33.70	33.10
11	-16.42	34.60	0.40	60.00	36.21	34.42	<b>36.20</b>	36.10	36.30	36.40
12	-16.79	33.60	0.60	60.00	36.07	35.28	<b>36.00</b>	36.10	36.20	36.30
13	-14.75	37.57	0.00	70.00	20.42	21.53	<b>20.40</b>	20.20	20.50	20.30
14	-15.40	36.45	0.20	70.00	24.32	24.41	<b>24.30</b>	24.20	24.40	24.10
15	-15.92	35.44	0.40	70.00	25.44	24.10	<b>25.50</b>	25.20	25.30	25.40
16	-16.29	34.46	0.60	70.00	25.32	25.33	<b>25.30</b>	25.10	25.20	25.50
<b>Statistical analysis</b>						R <sup>2</sup> =0.989 RSME = 0.831 MAPE = 2.056%	<b>R<sup>2</sup> = 0.998</b> <b>RMSE = 0.031</b> <b>MAPE = 0.078%</b>	R <sup>2</sup> =0.997 RMSE = 0.333 MAPE=0.668%	R <sup>2</sup> =0.996 RMSE = 0.441 MAPE = 0.717%	R <sup>2</sup> =0.997 RMSE = 0.277 MAPE = 0.612%

were set at the values shown in the figures. According to Gill et al. (2018c), the total irreversibility and 2nd law efficiency increased and decreased respectively with condenser temperature, when the refrigerant charge, condenser and evaporator temperatures were constant; this was due to increased irreversibility in the individual components and the total irreversibility respectively. This fact was further asserted in Fig. 15, in which the predictions of the ANFIS-SC model regarding the total irreversibility and 2nd law efficiency increase and decrease respectively with rise in condenser temperature, when other input parameters were held constant.

Furthermore, second law efficiency and total irreversibility of refrigeration system reduced and increased respectively with increasing evaporator temperature while maintaining constant refrigerant charge and condenser temperature, due to the increased irreversibilities of the system's sub-components (see Gill and Singh, 2018c). This was confirmed in Fig. 16, when the estimates of the ANFIS-SC model regarding the 2nd law efficiency and the total irreversibility of the domestic refrigeration system were reduced and increased respectively, by increasing the evaporator temperature while other parameters were fixed.

Additionally, the concentrations of nanoparticles in the nano-lubricant play a decisive role in the irreversibility analysis of

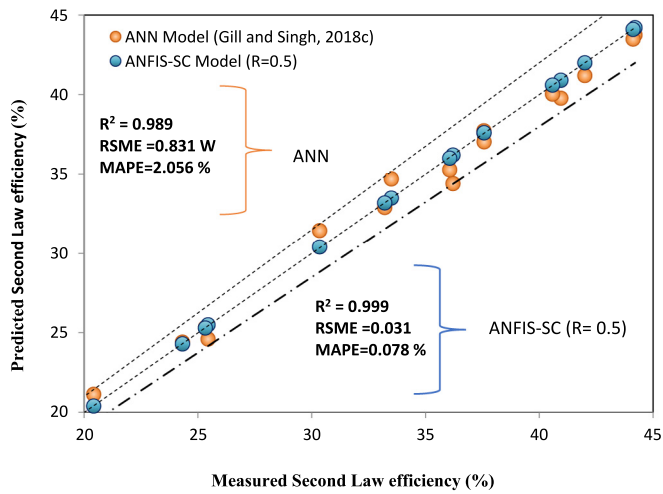


Fig. 8. ANN and ANFIS-SC models predictions of second law efficiency compared with corresponding experimental results.

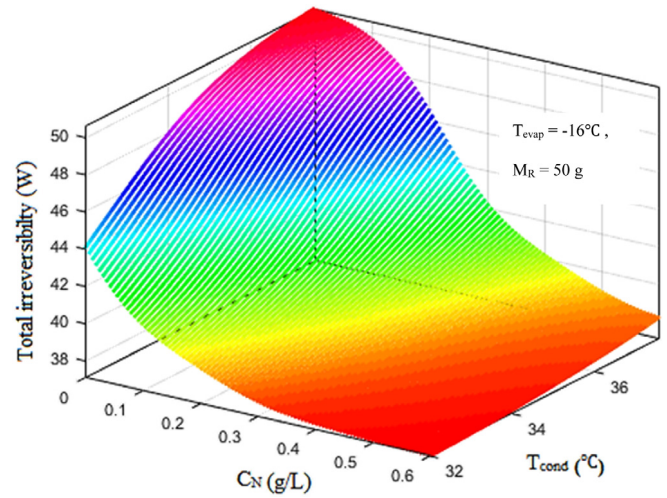


Fig. 11. Surface variation of ANFIS-SC model predictions of total irreversibility against the nanoparticle concentration and condenser temperature keeping other parameters fixed.

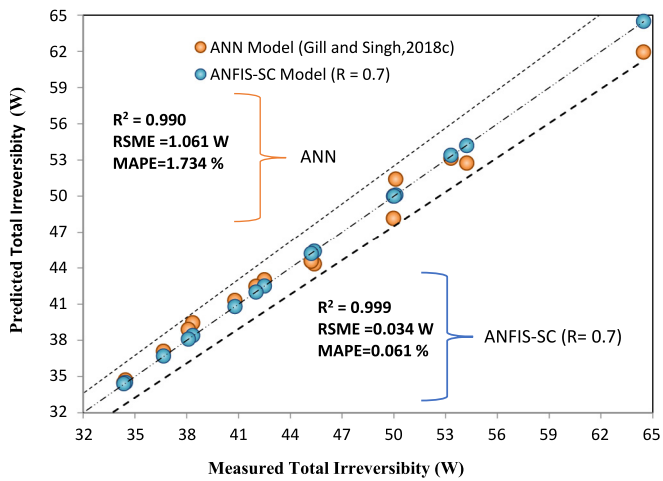


Fig. 9. ANN and ANFIS-SC models predictions of total irreversibility compared with corresponding experimental results.

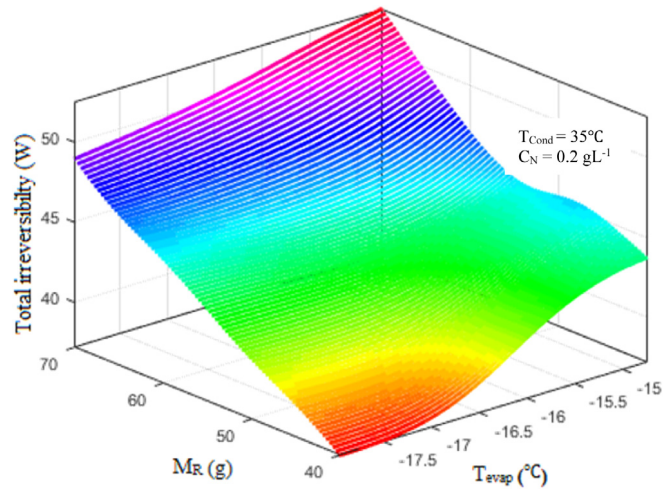


Fig. 12. Surface variation of ANFIS-SC model predictions of total irreversibility against the refrigerant charge and evaporator temperature keeping other parameters fixed.

domestic refrigeration system. The total irreversibility of domestic refrigerator system was decreased as we increase the concentration of  $TiO_2$  in nano-lubricant, due to reductions in the

irreversibility of the domestic refrigerator components (see Gill et al., 2018c). Moreover, the concentration of nanoparticle also

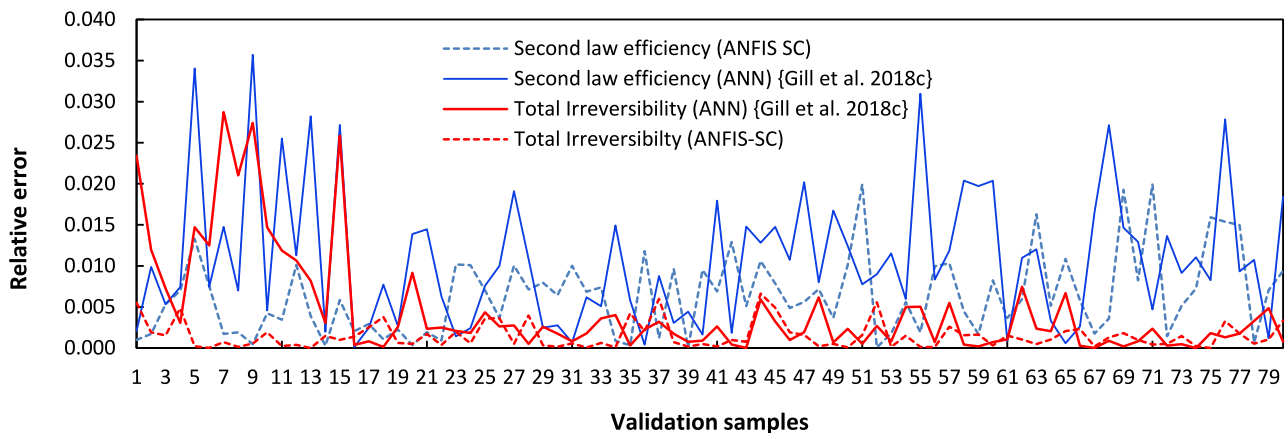
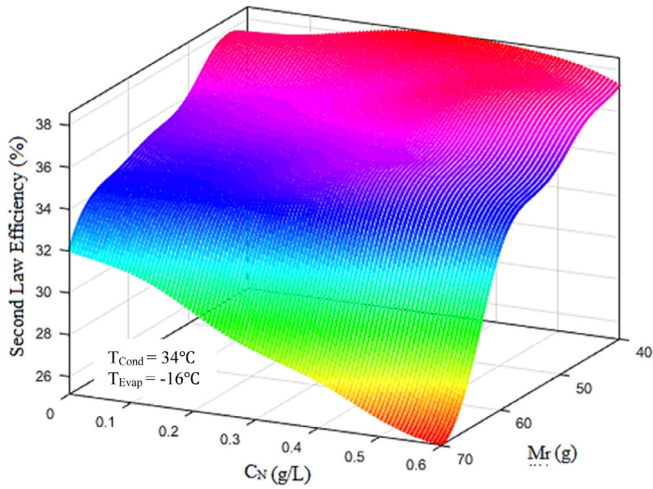
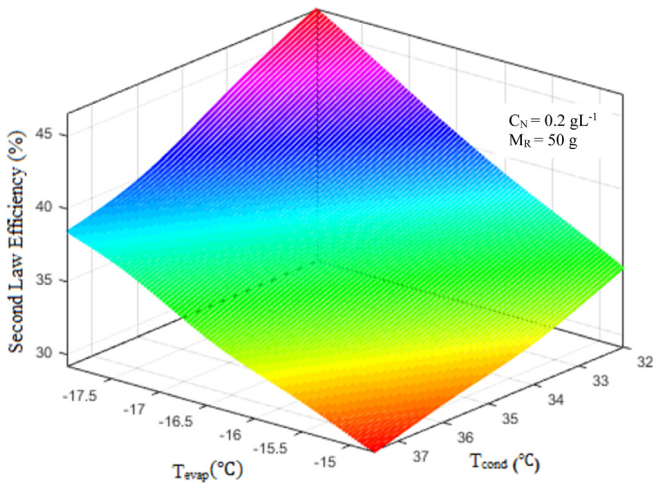


Fig. 10. Relative error comparison of the total irreversibility second law efficiency in accordance with the LOOCV for ANFIS-SC and ANN models. (For interpretation of the references to color in this figure legend, the reader is referred to the web version of this article.)



**Fig. 13.** Surface variation of ANFIS-SC model predictions of second law efficiency against the nanoparticle concentration and refrigerant charge keeping other parameters fixed.



**Fig. 14.** Surface variation of ANFIS-SC model predictions of second law efficiency against the evaporator and condenser temperature keeping other parameters fixed.

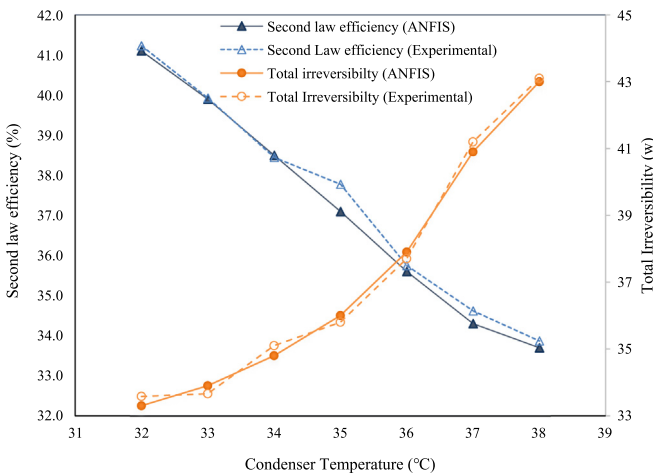


**Fig. 15.** Variation of ANFIS-SC model predictions of total irreversibility and second law efficiency along with corresponding experimental results against the condenser temperature keeping other parameters fixed.

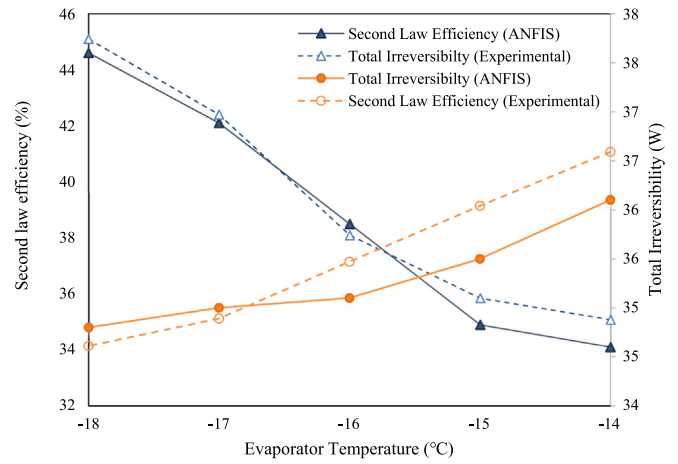


**Fig. 16.** Variation of predictions of ANFIS-SC model of the total irreversibility and second law efficiency along with corresponding experimental results against the evaporator temperature and keeping other parameters fixed.

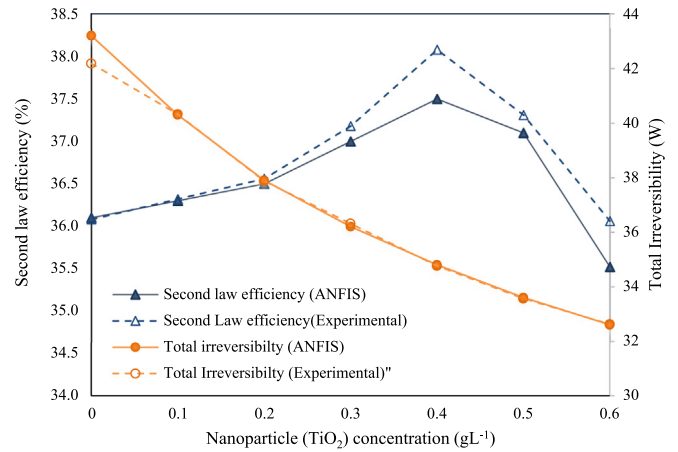


**Fig. 17.** Variation of ANFIS-SC model predictions of total irreversibility and second law efficiency along with corresponding experimental results against the nanoparticle concentration and keeping other parameters fixed.

influenced the second law efficiency; while keeping other parameters fixed, we found that the second law efficiency increased with increasing  $\text{TiO}_2$  concentration (i.e. from 0 to  $0.4 \text{ g L}^{-1}$ ) in the nano-lubricant. This happened because the rate of decrease in the total irreversibility was found to be more than the rate of decrease in the compressor power consumption, since the concentration of nanoparticles increased from 0 to  $0.4 \text{ g L}^{-1}$  (recalling the definition of second law efficiency). Nevertheless, the 2nd law efficiency decreased when concentration of  $\text{TiO}_2$  increases above  $0.4 \text{ g L}^{-1}$ , because rate of decrease of total irreversibility with respect to the rate of decrease of compressor power consumption was found less (See Table 6). Fig. 17 shows that the calculations of the ANFIS SC model correspond to the trend of the measured parameters of the total irreversibility and the 2nd law efficiency.

**5. Conclusions, limitation and future scope**

Using experimental data of author's previous publication Gill et al. (2018c), the ANFIS models were developed using Grid partition and Subtractive Clustering methodologies for predicting the total irreversibility and 2nd law efficiency of a refrigeration system infused with LPG refrigerant and  $\text{TiO}_2$ -MO nano-lubricant. The ANFIS models with subtractive clustering (ANFIS-SC) methodology were found more accurate than Grid partition



**Table 6**

Comparison of ANN and ANFIS-SC models predictions of total irreversibility with experimental results.

Sr No	Tevap (°C)	Tcond (°C)	C <sub>N</sub> (g L <sup>-1</sup> )	M <sub>R</sub> (g)	η(%)	I <sub>total</sub> (W)	W <sub>comp</sub> (W)	Reduction in I <sub>total</sub> (%)	Reduction in W <sub>comp</sub> (%)
1	-16	34	0	40	37.30	43.20	68.90	-	-
2	-16	34	0.1	40	37.60	40.30	64.58	6.71	6.26
3	-16	34	0.2	40	38.20	37.90	61.33	5.96	5.04
4	-16	34	0.3	40	38.50	36.20	58.86	4.49	4.02
5	-16	34	0.4	40	38.60	34.80	56.68	3.87	3.71
6	-16	34	0.5	40	38.20	33.60	54.37	3.45	4.07
7	-16	34	0.6	40	37.30	32.60	51.99	2.98	4.37

methodology. Additionally, results from the ANFIS-SC models were found closer to the experimental data in comparison to ANN model results developed by Gill et al. (2018c). However, the ANFIS model proposed in this publication may not give accurate results for other refrigerants and in operating conditions that are not within the range of the developed model. Furthermore, the accuracy of the developed ANFIS models can be further improved by using other refrigerant experimental data with different operating conditions for training purpose, since this publication used data from authors of previous publication only.

### CRedit authorship contribution statement

**Jatinder Gill:** Conceptualization, Methodology, Software, Writing - original draft. **Jagdev Singh:** Formal analysis. **Olayinka S. Ohunakin:** Data curation. **Damola S. Adelekan:** Software, Validation. **Opemipo E. Atiba:** Visualization. **Mojisola O. Nkiko:** Editing. **Aderemi A. Atayero:** Writing review.

### Declaration of competing interest

The authors declare that they have no known competing financial interests or personal relationships that could have appeared to influence the work reported in this paper.

### Acknowledgments

Authors of this work deeply appreciate the IKGPTU, Kapurthala, Punjab, India and Covenant University, Ogun State, Nigeria for their backing in funds and research capacities.

### References

- Adelekan, D.S., Ohunakin, O.S., Babarinde, T.O., Odufa, M.K., Leramo, R.O., Oyedepo, S.O., Badejo, D.C., 2017. Experimental performance of LPG refrigerant charges with varied concentration of TiO<sub>2</sub> nano-lubricants in a domestic refrigerator. *Case Stud. Therm. Eng.* 9–14.
- Ahamed, J.U., Saidur, R., Masjuki, H.H., 2010. Thermodynamic performance analysis of R-600 and R-600a as a refrigerant. *Eng. E-Trans.* 5, 11–18.
- Ahamed, J., Saidur, R., Masjuki, H., 2011. Prospect of hydrocarbon uses based on exergy analysis in the vapor compression refrigeration system. In: 2011 IEEE 1st Conference on Clean Energy and Technology (CET). IEEE, pp. 300–304.
- Akinlesi, L.J., Adelekan, D.S., Ohunakin, O.S., Atiba, O.E., Gill, J., Atayero, A.A., 2019. Experimental performance of a domestic refrigerator with TiO<sub>2</sub>-nanoparticles operating within selected ambient temperature. *J. Phys.: Conf. Ser.* 1378, 042081. <http://dx.doi.org/10.1088/1742-6596/1378/4/042081>, IOP Publishing.
- Belman-Flores, J.M., Ledesma, S., 2015. Statistical analysis of the energy performance of a refrigeration system working with R1234yf using artificial neural networks. *Appl. Therm. Eng.* 82, 8–17.
- Belman-Flores, J.M., Ledesma, S.E., Garcia, M.G., Ruiz, J., Rodriguez-Munoz, J.L., 2013. Analysis of a variable speed vapor compression system using artificial neural network. *Exp. Syst. Appl.* 40, 4362–4369.
- Esen, H., Inalli, M., Sengur, A., Esen, M., 2008. Performance prediction of a ground-coupled heat pump system using artificial neural networks. *Exp. Syst. Appl.* 35, 1940–1948.
- Gill, J., Ohunakin, O.S., Adelekan, D.S., Atiba, O.E., Ajulibe, B.D., Singh, J., Atayero, A.A., 2019. Performance of a domestic refrigerator using selected hydrocarbon working fluids and TiO<sub>2</sub>-MO nanolubricant. *Appl. Therm. Eng.* 160, 114004.
- Gill, J., Singh, J., 2017a. Energy analysis of vapor compression refrigeration system using mixture of R134a and LPG as refrigerant. *Int. J. Refrig.* 84, 287–299.
- Gill, J., Singh, J., 2017b. Experimental analysis of R134a/LPG as replacement of R134a in a vapor-compression refrigeration system. *Int. J. Refrig.* 1750015.
- Gill, J., Singh, J., 2017c. Energetic and exergetic performance analysis of the vapor compression refrigeration system using adaptive neuro-fuzzy inference system approach. *Exp. Ther. Fluid Sci.* 88, 246–260.
- Gill, J., Singh, J., 2017d. Adaptive neuro-fuzzy inference system approach to predict the mass flow rate of R134a/LPG refrigerant for straight and helical coiled adiabatic capillary tubes in the vapor compression refrigeration system. *Int. J. Refrig.* 78, 166–175.
- Gill, J., Singh, J., 2017e. Performance analysis of vapor compression refrigeration system using an adaptive neuro-fuzzy inference system. *Int. J. Refrig.* 82, 436–446.
- Gill, J., Singh, J., 2018a. Use of artificial neural network approach for depicting mass flow rate of R134a /LPG refrigerant through straight and helical coiled adiabatic capillary tubes of vapor compression refrigeration system. *Int. J. Refrig.* 86, 228–238.
- Gill, J., Singh, J., 2018b. An applicability of ANFIS approach for depicting energetic performance of VCRS using mixture of R134a and LPG as refrigerant. *Int. J. Refrig.* 85, 353–375.
- Gill, J., Singh, J., Ohunakin, O.S., Adelekan, D.S., 2018a. Energy analysis of a domestic refrigerator system with ANN using LPG/TiO<sub>2</sub>-lubricant as replacement for R134a. *J. Therm. Anal. Calor.* <http://dx.doi.org/10.1007/s10973-018-7327-3>.
- Gill, J., Singh, J., Ohunakin, O.S., Adelekan, D.S., 2018b. ANN approach for irreversibility analysis of vapor compression refrigeration system using R134a/LPG blend as replacement of R134a. *J. Therm. Anal. Calor.* <http://dx.doi.org/10.1007/s10973-018-7437-y>.
- Gill, J., Singh, J., Ohunakin, O.S., Adelekan, D.S., 2018c. Artificial neural network approach for irreversibility performance analysis of domestic refrigerator by utilizing LPG with TiO<sub>2</sub> -lubricant as replacement of R134a. *Int. J. Refrig.* 89, 159–176.
- Gill, J., Singh, J., Ohunakin, O.S., Adelekan, D.S., 2018d. Energetic and exergetic analysis of a domestic refrigerator system with LPG as a replacement for R134a refrigerant, using POE lubricant and mineral oil based TiO<sub>2</sub>-, SiO<sub>2</sub>- and Al<sub>2</sub>O<sub>3</sub>-lubricants. *Int. J. Refrig.* 91, 122–135.
- Golzari, S., Kasaian, A., Daviran, S., Mahian, O., Wongwises, S., Sahin, A.Z., 2017. Second law analysis of an automotive air conditioning system using HFO-1234yf, an environmentally friendly refrigerant. *Int. J. Refrig.* 73, 134–143.
- Guler, I., Ubeyle, E.D., 2005. Adaptive neuro-fuzzy inference system for classification of EEG signals using wavelet coefficients. *J. Neurosci. Methods* 148 (2), 113–121.
- Hosoz, M., Ertunc, H.M., 2016. Modelling of a cascade refrigeration system using artificial neural network. *Int. J. Energ. Res.* 30, 1200–1215.
- Hosoz, M., Ertunc, H.M., Bulgurcu, H., 2011. An adaptive neuro fuzzy inference system model for predicting the performance of a refrigeration system with a cooling tower. *Exp. Syst. Appl.* 38, 14148–14155.
- Jang, J.S., 1993. ANFIS: Adaptive-network-based fuzzy inference system. *IEEE Trans. Syst. Man Cybern.* 23, 665–685.
- Ledesma, S., Belman-Flores, J.M., 2014. Application of artificial neural networks for generation of energetic maps of a variable speed compression system working with R1234yf. *Appl. Therm. Eng.* 69, 105–112.
- Li, N., Xia, L., Shimming, D., Xu, X., Chan, M.Y., 2012. Steady-state operating performance modelling and prediction for a direct expansion air conditioning system using artificial neural network. *Build. Serv. Eng. Res. Technol.* 33, 281–292.
- Ohunakin, O.S., Adelekan, D.S., Babarinde, T.O., Leramo, R.O., Abam, F.I., Diarra, C.D., 2017. Experimental investigation of TiO<sub>2</sub>, SiO<sub>2</sub> and Al<sub>2</sub>O<sub>3</sub>-lubricants for a domestic refrigerator system using LPG as working fluid. *Appl. Therm. Eng.* 127.
- Ohunakin, O.S., Adelekan, D.S., Gill, J., Atayero, A.A., Atiba, O.E., Okokpujie, I.P., Abam, F.I., 2018. Performance of a hydrocarbon driven domestic refrigerator based on varying concentration of SiO<sub>2</sub> nano-lubricant. *Int. J. Refrig.* 94, 59–70.
- Okotie, T.E., Adelekan, D.S., Ohunakin, O.S., Gill, J., Atiba, O.E., Atayero, A.A., 2019. Performance evaluation of hydrocarbon based nanorefrigerants subjected to periodic door openings. *J. Phys.: Conf. Ser.* 1378, 042082. <http://dx.doi.org/10.1088/1742-6596/1378/4/042082>, IOP Publishing.



- Olatunji, O.R., Ohunakin, O.S., Adelekan, D.S., 2019. Effect of ambient temperatures on an R134a domestic refrigerator retrofitted with R600a and LPG refrigerants. *J. Phys.: Conf. Ser.* 1378, 022100. <http://dx.doi.org/10.1088/1742-6596/1378/2/022100>, IOP Publishing.
- Onakade, M.A., Adelekan, D.S., Ohunakin, O.S., Atiba, O.E., Gill, J., Atayero, A.A., 2019. Experimental performance of the energetic characteristics of a domestic refrigerator with Al<sub>2</sub>O<sub>3</sub> nanolubricant and LPG refrigerant. *J. Phys.: Conf. Ser.* 1378, 042083. <http://dx.doi.org/10.1088/1742-6596/1378/4/042083>, IOP Publishing.
- Onder, K., 2011. Thermodynamic analysis of a variable speed refrigeration system using artificial neural networks. *Exp. Syst. Appl.* 38, 11686–11692.
- Rashidi, M.M., Aghagoli, A., Raoofi, R., 2017. Thermodynamic analysis of the ejector refrigeration cycle using the artificial neural network. *Energ.* 129, 201–215.
- Raveendran, P.S., Sekhar, S.J., 2017. Exergy analysis of a domestic refrigerator with brazed plate heat exchanger as a condenser. *J. Therm. Anal. Calor.* 1–8.
- Saravanakumar, R., Selladurai, V., 2014. Exergy analysis of a domestic refrigerator using eco-friendly R290/R600a refrigerant mixture as an alternative to R134a. *J. Therm. Anal. Calor.* 115 (1), 933–940.
- Sowparnika, G.C., Thirumarimurugan, M., Sivakumar, V.M., 2015. Performance prediction of refrigeration systems by artificial neural networks. *Int. J. Adv. Res. Elect. Electron. Inst. Eng.* 4, 7673–7681.
- Tong, L., Yin, S., Xie, Y., Wang, L., Yue, X., Wang, G., 2010. Intelligent simulation on refrigeration system using artificial neural network. In: *Int. Conf. Nat. Comp.*, pp. 1709–1711.
- Yaici, W., Entchev, E., 2016. Adaptive neuro-fuzzy inference system modeling for performance prediction of solar thermal energy system. *Renew. Energy* 86, 302–315.